Functional analysis of a *de novo* variant in the neurodevelopment and generalized epilepsy disease gene *NBEA*

Thomas Boulin [a,1,2], Omar Itani [e,f,1], Sonia El Mouridi [a,1], Alice Leclercq-Blondel [a], Marie Gendrel [a,b], Ellen Macnamara [c], Ariane Soldatos [c], Jennifer L. Murphy [c], Mark P. Gorman [d], Anika Lindsey [e,f], Shino Shimada [c], Darian Turner [e,f], Gary A. Silverman [f], Dustin Baldridge [f], Undiagnosed Diseases Network, May C. Malicdan [c,2], Tim Schedl [e,g,2], Stephen C. Pak [e,f,2,*]

[a] Institut NeuroMyoGène, Univ Lyon, Université Claude Bernard Lyon 1, CNRS UMR 5310, INSERM U1217, Lyon 69008, France
[b] Institut de Biologie de l'Ecole Normale Supérieure (IBENS), Ecole Normale Supérieure, CNRS, INSERM, Université Paris Sciences et Lettres Research University, Paris 75005, France
[c] Undiagnosed Diseases Program Translational Laboratory, NHGRI, National Institutes of Health, Bethesda, MD 20892, USA
[d] Department of Neurology, Neuroimmunology Program, Boston Children's Hospital, Harvard Medical School, Boston, MA 02115, USA
[e] C. elegans Model Organism Screening Center, Washington University in St Louis School of Medicine, St Louis, MO 63110, USA
[f] Department of Pediatrics, Washington University in St Louis School of Medicine, St Louis, MO 63110, USA
[g] Department of Genetics, Washington University in St Louis School of Medicine, St Louis, MO 63110, USA

ARTICLE INFO

ABSTRACT

Neurobeachin (*NBEA*) was initially identified as a candidate gene for autism. Recently, variants in *NBEA* have been associated with neurodevelopmental delay and childhood epilepsy. Here, we report on a novel *NBEA* missense variant (c.5899G > A, p.Gly1967Arg) in the Domain of Unknown Function 1088 (DUF1088) identified in a child enrolled in the Undiagnosed Diseases Network (UDN), who presented with neurodevelopmental delay and seizures. Modeling of this variant in the *Caenorhabditis elegans NBEA* ortholog, *sel-2*, indicated that the variant was damaging to *in vivo* function as evidenced by altered cell fate determination and trafficking of potassium channels in neurons. The variant effect was indistinguishable from that of the reference null mutation suggesting that the variant is a strong hypomorph or a complete loss-of-function. Our experimental data provide strong support for the molecular diagnosis and pathogenicity of the *NBEA* p.Gly1967Arg variant and the importance of the DUF1088 for *NBEA* function.

1. Introduction

Neurobeachin, encoded by the *NBEA* gene, is a large (327 kDa), brain-enriched, multi-domain protein, that has been widely conserved during evolution. In *Drosophila*, mutants in the *NBEA* ortholog, *rugose,* have associative odor learning defects and abnormal synaptic architecture and physiology at larval neuromuscular junctions [1,2]. In zebrafish, Neurobeachin is required for both electrical and chemical synapse formation, and to maintain dendritic complexity [3]. In mammals, Neurobeachin has been implicated in vesicle trafficking and synaptic structure and function [3–7]. *Nbea* knockout neurons *in vitro* fail to develop a normal number of dendritic spines [5]. Neurobeachin contributes to the trafficking of membrane proteins to pre- and post-synaptic sites [8]. Notably, Neurobeachin binds the MAGUK protein SAP102 which is involved in trafficking of the ionotropic glutamate AMPA- and NMDA-type receptors during synaptogenesis [6] and *Nbea* knockout neurons are defective in glutamatergic and GABAergic synaptic transmission [9].

NBEA was initially identified as a candidate gene for autism based on linkage studies and the identification of structural variants (chromosomal microdeletions and reciprocal balanced translocations) at 13q13 in patients with autism [10–12]. Recently, *NBEA* was established as a rare cause of a complex neurodevelopmental disease associated with neurodevelopmental delay (NDD) and early generalized epilepsy based on the study of 24 affected individuals with *de novo* heterozygous variants (NEDEGE, OMIM #619157) [13]. Twenty of the 24 described cases were apparent heterozygous loss of function (8 nonsense, 5 frameshift, 5 intragenic deletions, 1 splice site, and 1 multigene deletion), which is congruent with *NBEA* being a haplo-insufficient gene (ClinGen; gnomAD v2.11). Four different *NBEA de novo* missense variants were also reported in this previous study [13], however, it is unclear to what extent gene function is disrupted as they are considered variants of uncertain significance (VUS). While clinical significance assessment

is challenging in such n-of-1 cases, experimental studies in model systems can provide important information on whether the missense variant disrupts gene function *in vivo* [14–16].

Here we report a proband admitted at the Undiagnosed Diseases Network (UDN) [17–19] with a novel *NBEA* missense variant (p. Gly1967Arg) in the Domain of Unknown Function 1088 (DUF1088) of Neurobeachin. Our proband had a neurodevelopmental disorder that presented with seizures and intellectual disability that was accompanied by pancreatitis and colitis. To determine the extent to which this novel variant disrupts gene activity, we performed *in vivo* functional analysis in the model organism *Caenorhabditis elegans* (*C. elegans*). We introduced the patient missense change into *sel-2*, the ortholog of Neurobeachin in *C. elegans*, using CRISPR/*Cas9* gene editing and assessed the impact of *sel-2* Gly1514Arg, corresponding to *NBEA* p.Gly1967Arg, using two *in vivo* assays that test the functionality of SEL-2. We provide data demonstrating that *sel-2* Gly1514Arg is functionally damaging and most likely a loss-of-function mutation [20], lending strong support for the molecular diagnosis and pathogenicity of the *NBEA* p.Gly1967Arg variant.

2. Materials and methods

2.1. Proband evaluation and consent

Informed consent for the participation in the study, clinical data and specimen collection, genetic analysis and publication of relevant findings was obtained from parents of the subject. Procedures were followed in accordance with guidelines specified by Institutional Review Boards (IRB) and Ethics Committees of each institution. The Undiagnosed Diseases Network (UDN) protocol, 15-HG-0130, was approved by the National Human Genome Research Institute IRB. Permission to publish photographs was provided. The proband was seen at the NIH Undiagnosed Diseases Program, one of the clinical sites of the UDN.

2.2. Genome sequencing

Genomic DNA was prepared from peripheral blood obtained from the proband and members of his family, using approved clinical methods. Clinical genome sequencing was performed by Hudson Alpha (Huntsville, AL) using the Illumina HiSeq X sequencing platform. After sequencing, reads were generated using Illumina's bcl2fastq and data were aligned to hg19 (GRCh37). Patient sequence variants were loaded into a custom software analysis application, Carpe Novo, for interpretation. Within Carpe Novo all sequence variants are annotated with relevant reference information from established data sources to provide support for interpretation. For research analysis, fastq sequencing data were aligned to human reference assembly hg19 (GRCh37), followed by variant calling and joint genotyping using the Illumina DRAGEN Biosingle bondIT Platform (v2.6). The VCF file was annotated using the Variant Effect Predictor (VEP v95) and vcfanno (v0.2.9), and Gemini (v0.20.1) was used to query variants of interest. Each variant was filtered for gnomAD population frequency < 1%. Sanger sequencing was performed to validate findings. Of note, research reanalysis was performed during the time of the initial publication when the *NBEA* was associated with epilepsy in 2018.

2.3. C. elegans genetics

Worms were raised at 20 °C on nematode growth medium and fed *Escherichia coli* OP50 [21]. Strains generated for this study are listed in Supplementary Table S1. *sel-2* and *lin-12* are tightly linked (~1 cM). *Cis* double recombinants of *sel-2 udn#* allele and *lin-12(n302)* were recovered by generating trans-heterozygotes and screening F2 segregants for the recombinant molecular genotype. Strains containing *sel-2 udn#* allele (chromosome III) and *egl-23::wrmScarlet* (chromosome IV) were generated by standard segregation analysis.

2.4. Orthology

In vertebrate species, *NBEA* has a paralog called *LRBA*, where the gene duplication arose at the split between the vertebrate and invertebrate lineages [22]. While *sel-2* is ancestral in sequence to both *NBEA* and *LRBA*, it is orthologous to *NBEA* based on a number of sequence relatedness metrics (14/15 DIOPT score and best forward and reverse score; https://www.flyrnai.org/diopt), suggesting that *LRBA* diverged after the duplication. *NBEA* primarily functions in the nervous system, while *LRBA* primarily functions outside the nervous system [23]. *sel-2* is apparently also ancestral in site of action as it functions in both the nervous system in ion channel localization (this study) and functions outside the nervous system in the regulation of cell fate [24].

2.5. Molecular biology

Single-strand oligonucleotides used for this study are described in Supplementary Table 2. Whole-genome sequencing was performed on purified genomic DNA (DNEasy, Qiagen) by a commercial service provider (GATC Biotech) using Illumina HiSeq sequencing technology. An in-house software pipeline was used to analyze raw sequencing data and predict deleterious polymorphisms.

2.6. CRISPR/Cas9-based gene editing and miniMos transgenesis

sel-2 variant-edited alleles *udn20-22* and control-edited alleles *udn23-24* were generated by RNP-based CRISPR/*Cas9* gene editing [25] using the crRNA, TTTATTGAGCTTGTGAACGA, and single-strand oligonucleotide repair templates oUDN173 and oUDN174 for variant and control edits, respectively (Supplementary Fig. S2 and Supplementary Table S2). *udn20-24* alleles were genotyped using *SpeI* restriction length polymorphism of a 449 bp-long oTB700/oTB701 PCR fragment (Supplementary Table S2). Sanger sequencing was used to verify each of the edited alleles. Observing essentially identical phenotypes in the vulval cell fate determination and potassium channel trafficking assays for the independent variant-edited lines, while failing to observe a phenotype in the control-edited lines, demonstrates that the damaging phenotype can be specifically attributed to the variant edit.

The transcriptional reporter *blnTi1* labeling IL1DL/R and IL1VL/R was generated using *miniMos* transgenesis [26] with the plasmid pSEM159, which drives expression of GFP using a 584 bp long promotor fragment of *flp-3* spanning from 5′-agaaactctggccgcaataaaagag-3′ to 5′-gatatcgttggtggttatggtggtgttac-3′.

The N-terminal translational reporter fusion allele *sel-2(bln344 [wrmScarlet::sel-2])* was generated using the CRpSEM94 single-guide RNA (TTTTTCAGAGATTATTTGAA) expression vector [27] and pSEM115 repair template, which contains a wrmScarlet-3xFLAG cDNA sequence and a self-excising selection cassette [28]. The proband variant G1514R and synonymous changes in *udn20-22* were engineered into this background by CRISPR/*Cas9*-based gene editing using the same reagents as above (Supplementary Fig. S2 and Supplementary Table S2) to produce *sel-2(bln344bln893)*.

2.7. Visual screen for mutants with altered EGL-23 enrichment in IL1 neurons

egl-23::TagRFP-T (JIP1175) worms were mutagenized with EMS, and single F1 progeny were cloned to fresh plates. In the F2 generation, one-day old adult hermaphrodites were transferred to 24-well plates (2% agarose in water, 1% sodium azide, per well) and screened on an AZ100 macroscope (Nikon) equipped with a Flash 4.0 CMOS camera (Hamamatsu Photonics). Candidate mutants with defects in EGL-23-TagRFP-T enrichment in IL1 dendrites were subsequently isolated from the F1 clonal plate and causative mutations in *sel-2* identified by whole-genome sequencing.

2.8. Quantification of EGL-23 enrichment in IL neurons

EGL-23-wrmScarlet fluorescence was measured using an AZ100 macroscope (Nikon) equipped with a Flash 4 CMOS camera (Hamamatsu). Worms were immobilized using polystyrene beads (2%, in M9 buffer) on dry 2% agarose pads. Identical regions of interest (ROI) were selected in all genotypes, corresponding to the most anterior portion of the IL dendrites, and total fluorescence measured with identical imaging settings. Background fluorescence was subtracted by averaging the fluorescence intensity of equivalent ROIs surrounding the tip of the head of each worm.

2.9. Confocal microscopy

Confocal imaging was performed using an inverted confocal microscope (Olympus IX83) equipped with a CSU spinning-disk scan head (Yogokawa) and an EMCCD camera (iXon ultra 888). Worms were imaged on 2% fresh agar pads mounted in M9 solution containing 50 mM sodium azide.

2.10. Data availability statement

The data that support the findings of this study are available from the corresponding author upon request.

3. Results

3.1. Clinical report

Our proband is a six-year-old female who presented with epilepsy, global developmental delay, and ataxia. She was enrolled in the Undiagnosed Diseases Network protocol, 15-HG-0130, which is approved by the NIH National Human Genome Research Institute Institutional Review Board (IRB), and was seen at the NIH Clinical Center. Informed consent for this study was obtained from the proband's parent. Comprehensive biochemical and genetic workup, including metabolic screening, mitochondrial studies and DNA analysis, multiple gene panel sequencing, and clinical exome sequencing did not provide a diagnosis. During admission, pertinent neurological findings included left ptosis, dysarthria, and appendicular hypotonia. She had mild to moderate intellectual disability and because of the suspicion of autism spectrum disorder (ASD), a formal psychological evaluation concluded that she did not meet the criteria for ASD. On brain magnetic resonance imaging (MRI), she had mild cortical atrophy and punctate sub-cortical white matter T2 hyperintensities (Fig. 1a, Supplementary Fig. S1). Further details of the clinical history and findings are presented in the Supplementary Clinical Report. Clinical genome sequencing of DNA from the proband and her parents were also nondiagnostic. Of note, clinical genome sequencing was performed in 2016. Research reanalysis in 2018 revealed a *de novo* missense variant (c.5899G > A, p.Gly1967Arg) in *NBEA*, which was later confirmed by Sanger sequencing by a clinical diagnostic laboratory.

3.2. Conservation of Gly1967 and the DUF1088 domain in C. elegans

To evaluate the effect of p.Gly1967Arg on *NBEA* activity in our UDN proband, we tested the functional impact of this variant in the model organism, *C. elegans*. The *C. elegans* ortholog of *NBEA* is *sel-2*. It shares all the known protein domains of vertebrate Neurobeachin (Fig. 1b) and has high overall sequence conservation ranging from 35% to 65% identity in recognizable protein domains [24]. The Gly1967Arg variant is located at the N-terminus of the DUF1088 domain. Overall conservation of the DUF1088 domain is high, in particular around Gly1967 (Fig. 1c). This allowed us to precisely reproduce the Gly1967Arg variant in the corresponding *C. elegans* residue (Gly1514) of SEL-2 using CRISPR/Cas9-based gene editing. As part of our editing strategy, we also introduced

synonymous changes that block Cas9 re-cleavage following homology-directed repair and generate a restriction enzyme cleavage site used for allele genotyping (Fig. S2). Therefore, to use as controls, we generated lines that only contain the synonymous and restriction enzyme changes, but not the proband's variant. In total, we generated three independent alleles with the variant edit and two independent control edit alleles that do not change the variant residue (Supplementary Table S1). All of these edited lines were superficially wild-type, similar to *sel-2* null mutants.

3.3. SEL-2 Gly1514Arg disrupts cell fate induction via the notch signaling pathway

In *C. elegans*, SEL-2 plays a modulatory role in LIN-12/Notch signaling during cell fate decisions leading to the proper formation of the vulva. Notch signaling promotes the secondary vulval cell fate [29], and SEL-2 acts as a negative regulator by restricting the Notch receptor to the apical membrane of epidermal cells that can undergo vulval cell fate specification [24]. This negative regulatory function can be revealed by a genetic interaction test using the weak *lin-12* gain-of-function allele, *n302*. The *lin-12(n302)* allele is almost completely wild-type on its own (Fig. 2a, top left panel and Table 1). However, when it is combined with the *sel-2* canonical null mutation (*ar219*), worms display ectopic secondary vulval cell fate specification leading to a characteristic multi-vulva (Muv) phenotype [24] (yellow arrowheads, Fig. 2a, bottom left panel and Table 1).

We found that the proband's variant strongly enhanced the *lin-12 (n302)* multi-vulva phenotype (81–82%) (Fig. 2a, bottom right panel and Table 1). Notably, it did so to a similar extent as the null allele *sel-2(ar219)* (71%, Table 1). In contrast, the control-edited allele did not enhance *lin-12(n302)* (0%, Table 1). Additionally, as observed for *sel-2* null mutants, the proband's variant did not cause a multi-vulva phenotype on its own (*i.e.*, in a *lin-12(+)* wild-type background) (Table 1). These results clearly indicate that SEL-2 Gly1514Arg is defective in its function as a negative regulator of LIN-12 signaling. Strikingly, given the similar magnitude of the multi-vulva phenotype, the proband's variant is as defective as the reference nonsense allele *ar219*, although it carries only the single Gly1514Arg amino acid change.

3.4. SEL-2 Gly1514Arg is defective in localization of the two-pore domain potassium channel EGL-23 to dendritic termini

Two-pore domain potassium (K2P) channels are members of a large family of conserved ion channels that play a central role in the establishment and maintenance of the resting membrane potential and therefore regulate neuronal excitability [30]. The *C. elegans* genome encodes 47 K2P channel subunits [31], expressed in different cell types. Systematic tagging of K2P channels using CRISPR/Cas9 gene-editing showed that the EGL-23 channel was expressed in a subset of polymodal neurons, called inner labial IL neurons (manuscript in preparation). Specifically, EGL-23 is expressed prominently in four IL1 (IL1DL/R and IL1VL/R) and two IL2 (IL2L and IL2R) neurons (Fig. 2b). These neurons are situated in the head of the worm and project dendrites anteriorly into the tip of the worm's nose. Tagging EGL-23 with the red fluorescent protein, wrmScarlet [27], revealed that these channels are enriched at the extremities of these dendrites (Fig. 2b, ROI, dashed squares). This striking localization prompted us to search for genes that promote dendritic terminal localization using a genetic screen for mutants with decreased fluorescence levels at dendritic termini. In a pilot screen using random chemical mutagenesis, we isolated two independent mutants (*bln289* and *bln291*, Fig. 1b) that showed such a phenotype and identified them as alleles of *sel-2/NBEA* using whole-genome sequencing.

By fluorescence quantification, we found that the *sel-2* mutation caused an approximate 50% decrease in mean fluorescence intensity at the tip of sensory dendrites (Fig. 2c). Note that some of the residual EGL-23-wrmScarlet fluorescence can be explained by the presence of
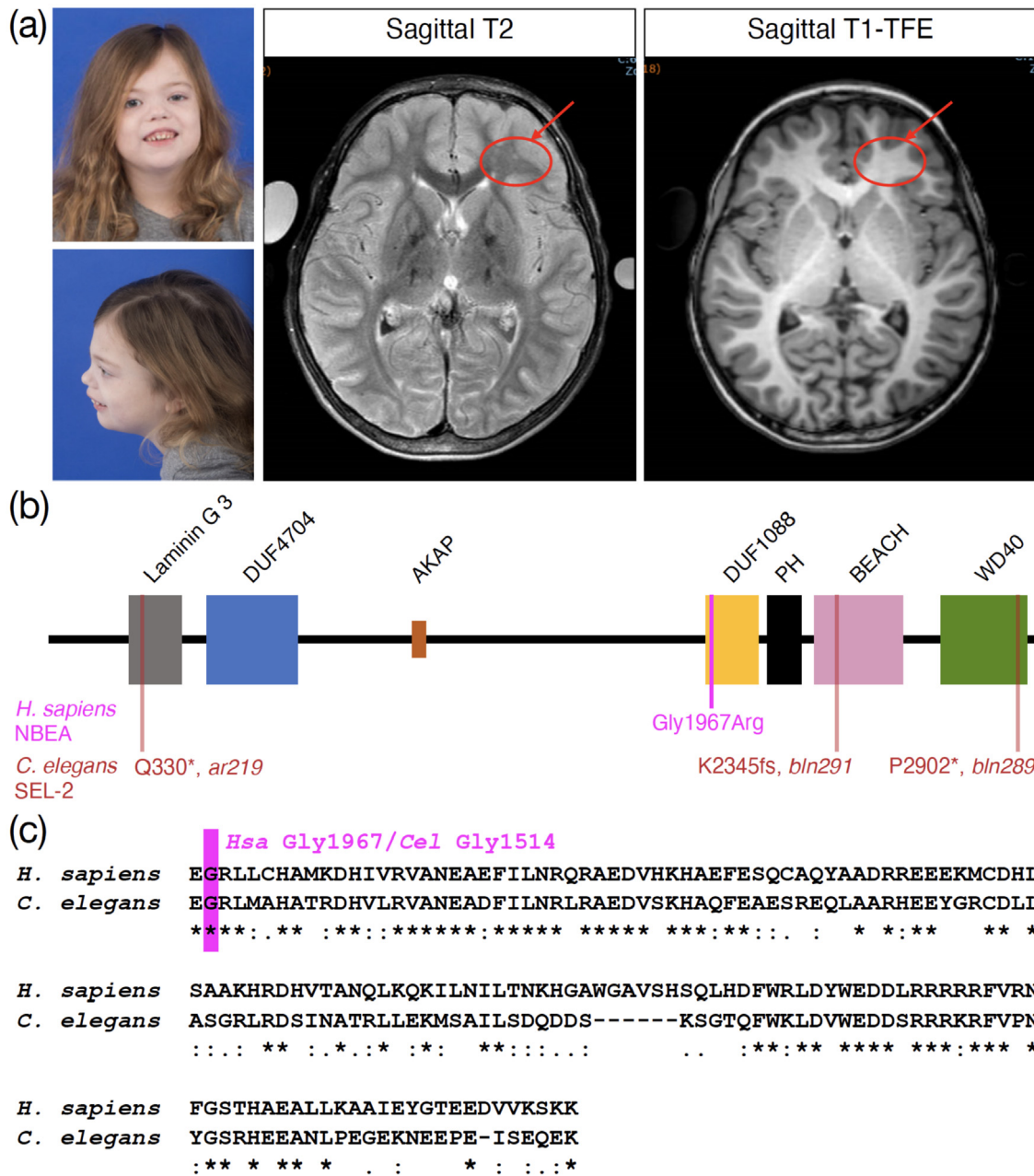
Fig. 1. Proband with a *de novo NBEA* variant and conservation of Gly1967 in the DUF1088 domain of human Neurobeachin and *C. elegans* SEL-2. (a) Left panel shows photographs of the proband with left ptosis, and absence of distinct facial dysmorphology. Right panel shows representative axial brain magnetic resonance imaging photos (MRI) that demonstrates the T2 hyperintensities (encircled in red, arrow), which are not observed in corresponding T1-weighted images. Also note the presence of mild cortical atrophy, which is more evident in T1-weighted turbo field echo sequence. These brain MRI photos were taken at the age of 6. (b) Domain composition of Neurobeachin. Proband variant is shown in pink. *C. elegans* alleles are shown in dark red. (c) Sequence comparison of human Neurobeachin and *C. elegans* SEL-2 DUF1088 domains. Residue p.Gly1967 is conserved at position p.Gly1514 in SEL-2.

EGL-23 in the adjacent IL2 dendrites (Fig. 2b and d), suggesting a reduction that is likely even higher than 2-fold in affected IL1 neurons.

Using this functional assay, we tested the impact of the Gly1514Arg variant identified in our proband and control edits by crossing the EGL-23-wrmScarlet translational reporter into the edited strains (Fig. 2d). We observed a marked reduction in channel accumulation in the dendritic termini of IL1 neurons with all three *sel-2* Gly1514Arg alleles (*udn20, udn21,* and *udn22*; Fig. 2d and e). Conversely, the Gly1514Gly control edits (*udn23* and *udn24*) had no impact on channel accumulation. This 2-fold reduction in EGL-23-wrmScarlet fluorescence in the variant-edited strains is similar to the effect observed with *sel-2* loss-of-function mutants (Fig. 2c and f).

Taken together, these results reveal that Gly1514Arg leads to defective *sel-2* function with a severity that is indistinguishable from that of *sel-2* null mutants, lending strong support for the genotype to phenotype linkage in the patient. Additionally, this work provides the first experimental evidence for the importance of the DUF1088 domain for SEL-2 and likely Neurobeachin function.

3.5. SEL-2 null and variant-edited mutants are weakly haplo-insufficient

Dominant loss of function presentation [13] and strong selection against heterozygous loss of function variants in the human population (gnomAD v2.11) indicates that *NBEA* NEDEGE (OMIM #619157) cases
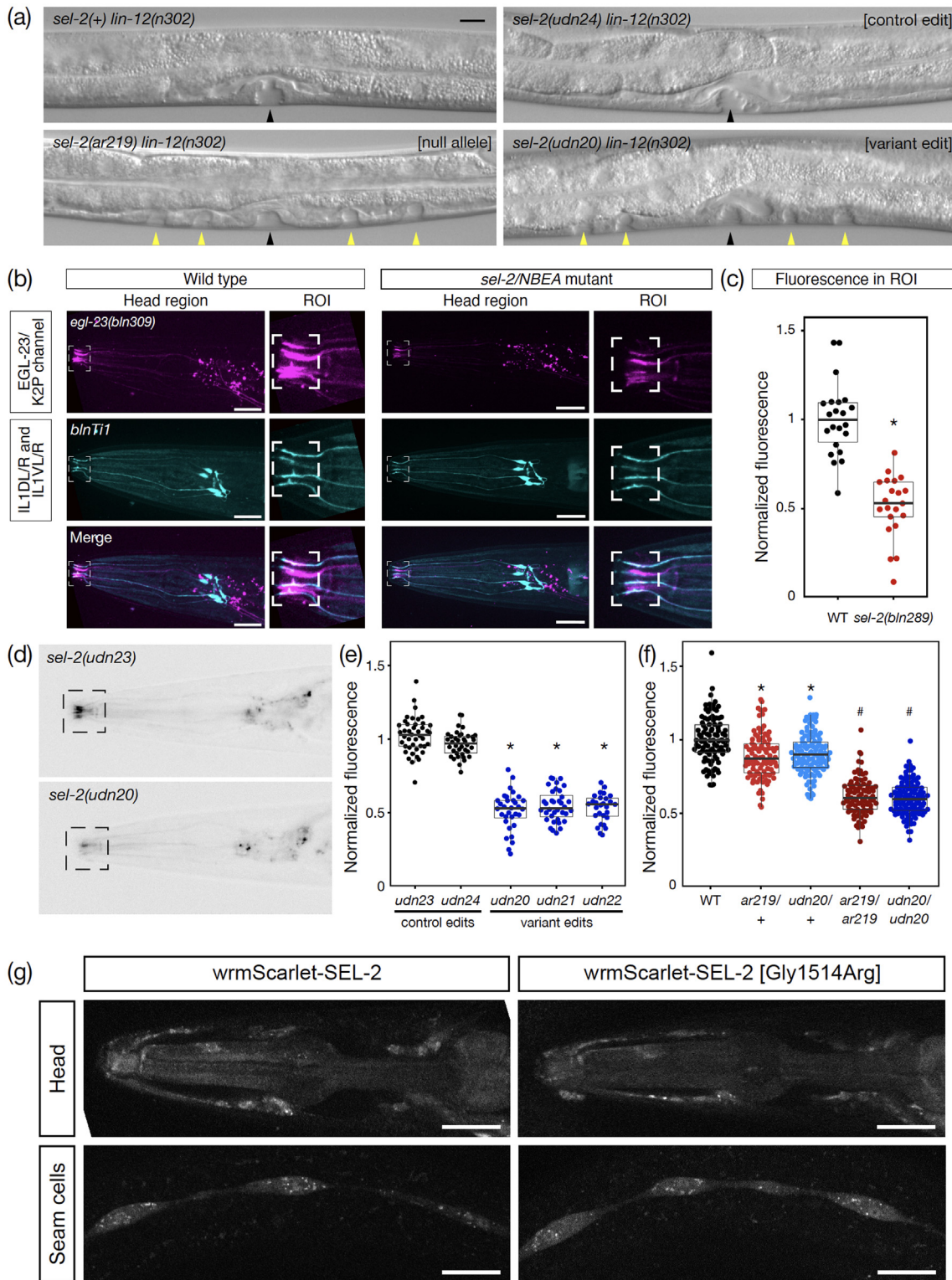
Fig. 2. Modeling of *NBEA* Gly1967 variant in *C. elegans* SEL-2. (a) *sel-2* variants enhance the multi-vulva (Muv) phenotype of *lin-12(n302)* gain-of-function. Increased LIN-12 signaling in vulval precursor cells leads to the formation of vulval (black arrowheads) and pseudovulval invaginations (yellow arrowheads), which will give rise to ectopic vulva in adults, in *sel-2* reference null (*ar219*) and variant edit (*udn20*) animals. *lin-12-12(n302)* alone or control edits (*udn24*) combined with *lin-12(n302)* show little to no phenotype. Nomarski differential interference contrast microscopy images of mid-L4 stage hermaphrodites, anterior to the left, ventral surface below. Scale bar, 20 μm. (b) SEL-2 is required for EGL-23 accumulation at the tip of IL1 dendrites. *egl-23(bln309)* is a C-terminal translational fusion of EGL-23 with wrmScarlet (magenta). *blnTi1* is a transgenic reporter expressing GFP exclusively in IL1DL/R and IL1VL/R using a minimal *flp-3* promoter (cyan). In a *sel-2* loss-of-function mutant, EGL-23-associated fluorescence is reduced by approx. 50% at dendritic termini (compare magenta in dashed rectangles; ROI, Region of interest). EGL-23 remains enriched at the termini of IL2L/R neurons. (c) Significant decrease of fluorescence intensity in region of interest in a *sel-2(bln289)* loss-of-function mutant. Each data point represents one animal, $n > 21$. Student's *t*-test, * $P < 0.01$. (d) The patient variant corresponding to *sel-2* p.Gly1514Arg decreases EGL-23 channel density at the tip of IL1 dendrites. EGL-23-wrmScarlet fluorescence is markedly reduced in *sel-2(udn20)* carrying the variant edit Gly1514Arg compared to the control-edited *sel-2(udn23)*. Region of interest, dashed square. (e) 2-fold reduction in normalized fluorescence intensity in region of interest of three variant-edited alleles (*udn20, udn21, udn22*) compared to control-edited *sel-2* alleles (*udn23, udn24*). Each data point is one animal. $n > 28$. One-Way Anova, with Tukey HSD test * $P < 0.01$. (f) Intermediate reduction in normalized fluorescence intensity for heterozygous *ar219* null and *udn20* patient variants compared to wild-type and homozygous mutants. Each data point is one animal. $n > 87$. Student's t-test with Bonferroni multiple comparison adjustment. WT *vs.* heterozygotes, * $P < 0.01$. Heterozygotes *vs.* homozygotes, # $P < 0.01$. (g) wrmScarlet-SEL-2 expression levels and subcellular localisation in muscle, neurons and epithelial cells is not altered by the p.Gly1514Arg patient variant. Scale bar, 20 μm.

Table 1
Quantification of multi-vulva (Muv) phenotype in *sel-2* variants.

	Allele type	Genotype	%Muv[†,§]	Avg # pseudo-vulvae[‡]	Sample size
a	wild-type	*sel-2(+) lin-12(n302)*	1	0.04	100
b	null allele	*sel-2(ar219[stop])lin-12(n302)*	71	3.19	100
c	control edit	*sel-2(udn24[G > G])lin-12(n302)*	0	0	100
d	variant edit #1	*sel-2(udn20[G > R])lin-12(n302)*	81	3.09	117
e	variant edit #2	*sel-2(udn21[G > R])lin-12(n302)*	82	2.58	100
	variant edit #1	*sel-2(udn20[G > R])lin-12(+)*	0	0	>100
	variant edit #2	*sel-2(udn21[G > R])lin-12(+)*	0	0	>100

[†] Muv = 2 or more pseudovulvae, scored as 1-day old adults.

[‡] Total number of pseudovulvae divided by number of worms.

[§] *a-b* Muv comparison, significantly different $p < 0.00001$, Chi-squared test.

[§] *a-c* Muv comparison, not significant.

[§] *c-d* Muv comparison, significantly different $p < 0.00001$.

[§] *c-e* Muv comparison, significantly different $p < 0.00001$.

[§] *d-e* Muv comparison, not significant.

The cis recombinant between *sel-2(udn22)* and *lin-12(n302)* was not generated, and thus not analyzed.

arise by a haploinsufficient genetic mechanism. However, it is possible that p.Gly1967Arg may act by a dominant negative mechanism. We, therefore, used the EGL-23-wrmScarlet fluorescence assay to compare heterozygotes and homozygotes for null and proband alleles (Fig. 2f). We found that the level of fluorescence in null mutant heterozygotes (*ar219/+*) was significantly less than wild-type but more than in homozygous mutants (Fig. 2f), indicating that *sel-2* is a haploinsufficient gene in *C. elegans*, as is its ortholog in humans. If the variant results in a dominant negative effect, we expect variant heterozygotes to show a further reduction in fluorescence level compared to null heterozygotes. Instead, we found that variant heterozygotes (*udn20/+*) were indistinguishable in the level of fluorescence reduction from the null heterozygotes (*ar219/+*) (Fig. 2f), consistent with the variant being a strong hypomorph or complete loss of function, rather than a dominant negative.

3.6. SEL-2 protein levels and subcellular localisation are unchanged by Gly1514Arg

The subcellular localisation and expression levels of SEL-2 have not been reported to date. To visualize SEL-2 *in vivo*, we used gene editing to produce a translational knockin line in which wrmScarlet is fused to the amino terminus of SEL-2 (Fig. 2g, Supplementary Fig. S3). Consistent with single-cell RNAseq data [32], we found that SEL-2 was broadly expressed in muscles, neurons and epithelial cells. In neurons and epithelial seam cells, we observed diffuse fluorescence, in addition to discrete fluorescent puncta in the soma (Fig. 2g). To determine the impact of the patient variant on SEL-2 protein levels or subcellular distribution, we used gene editing to incorporate the Gly1514Arg patient variant into this SEL-2 translational reporter. Overall expression and specific enrichment in somatic puncta were unchanged in these mutant lines compared to wild-type, indicating that the Gly1514Arg mutation does not lead to a destabilization of SEL-2 or alteration of its expression level (Fig. 2g). These data suggest that the patient mutation may interfere with a specific function of the DUF1088 domain.

4. Discussion

Trio exome sequencing identified the *NBEA* heterozygous *de novo* missense p.Gly1967Arg variant of uncertain significance in case UDN438089, who presented with NDD and epilepsy phenotypes that are similar to those previously described for loss of function variants in *NBEA* [13]. Here we report robust experimental data from modeling p.Gly1967Arg in the *C. elegans* ortholog *sel-2* that the variant is damaging to function *in vivo*. Employing two distinct biological readouts, the variant effect is indistinguishable from complete *sel-2* loss-of-function. By extension, the functional data suggests that *NBEA* p.Gly1967Arg is damaging, likely resulting in strong hypomorphic or complete loss of

function. The functional data, combined with the *in silico* prediction of likely deleterious (CADD score 31), the absence of variants at residue p.Gly1967 in control population databases (gnomAD v2.11 and 1000G), and UDN438089 presentation that overlaps with previous reports, are all consistent with an haplo-insufficient mechanism for the NDD and epilepsy phenotypes in *NBEA* disease [13,33].

A number of *NBEA* missense variants have been reported in patients with autism, NDD or epilepsy [13,34,35], however, they have not been functionally validated. These *in vivo* assays in *C. elegans* will offer a rapid, inexpensive and quantitative method to ascertain the functional effect of these and future *de novo* mutations identified in *NBEA*.

Given its large size and modular organization, Neurobeachin is likely a molecular scaffold that supports numerous protein-protein interactions. As variants from affected individuals are found throughout the protein, these missense mutations can also provide valuable information about key functional domains, since they might disrupt specific protein-protein interactions, or alter only some functions of the protein, thus genetically separating the different roles of such large modular proteins. For example, a single point mutation in the PH domain specifically disrupts the binding of the MAGUK protein and SAP102 to Neurobeachin [6]. Conversely, it is useful to understand whether protein domains have specific functions when trying to predict the possible molecular and cellular consequences of variants identified in affected individuals. Indeed, individual domains are sufficient to restore spine density and AMPA receptor surface targeting (PH-BEACH), filopodia formation (Armadillo/DUF4704 domain), or negative regulation of filopodia extension (PKA-binding domain) in Neurobeachin deficient neurons [36].

Here, we provide the first genetic data in support of the importance of DUF1088 for SEL-2 and likely Neurobeachin function. DUF1088 domains are exclusively found in Neurobeachins and their homologs, but there is very limited data about their function. A previous report has suggested that DUF1088 domains harbor a nuclear localization signal consisting of a poly-arginine stretch [37]. Gly1967 is not located close to this sequence in the primary protein sequence, but structural data is lacking to determine the precise organization of DUF1088. It will be informative to identify molecular interactors of DUF1088 domains to better understand if variants in this domain could disrupt specific Neurobeachin functions.

Our experimental studies in *C. elegans* showed that *sel-2* Gly1514Arg is damaging to function both in negative regulation of LIN-12/Notch signaling in epidermal cells and in terminal dendritic localization of the EGL-23 K2P channel in IL1 neurons. Interestingly, these functional deficits both involve defective accumulation of transmembrane proteins in the appropriate subcellular compartment. Indeed, the redistribution of LIN-12/Notch receptors to the basolateral domain of vulval precursor cell (VPC) in *sel-2* mutants is thought to explain the increase in LIN-12/Notch signaling and associated cell fate changes [24], although the

precise cellular mechanism that causes this redistribution remains to be determined.

In mammals, Neurobeachin has been implicated in vesicle trafficking and synaptic targeting of ionotropic glutamate, GABA, and glycine receptors [7,9,36,38]. Our data provide the first functional link between SEL-2/Neurobeachin and a two-pore domain potassium channel. It is thus possible that, in addition to ligand-gated ion channels, Neurobeachin may also regulate K2P channels and other classes of ion channels involved in neuronal excitability. Notably, mutations in K2P channels have recently been linked with rare neurological diseases. Birk Barel intellectual disability with dysmorphism syndrome is caused by a mutation in TASK3/ *KCNK9* [39,40]. This maternally transmitted syndrome presents with intellectual disability, hypotonia and specific dysmorphism of the face.

Impairment of broadly-acting cellular regulators such as SEL-2/ Neurobeachin that control the subcellular trafficking and localization of different ion channels and membrane proteins may therefore impinge on multiple pathways at once. Additionally, it is possible that specific missense variants may alter only some Neurobeachin functions, leading to more restricted clinical presentation. Systematic functional studies of Neurobeachin variants will be important to develop a better understanding of the genotype to phenotype relationships in Neurobeachin disease.

Supplementary data to this article can be found online at https://doi.org/10.1016/j.ymgme.2021.07.013.

CONSORTIA (members of the undiagnosed diseases network)

Maria *T. Acosta*, Margaret Adam, David R. Adams, Pankaj B. Agrawal, Mercedes E. Alejandro, Justin Alvey, Laura Amendola, Ashley Andrews, Euan A. Ashley, Mahshid S. Azamian, Carlos A. Bacino, Guney Bademci, Eva Baker, Ashok Balasubramanyam, Dustin Baldridge, Jim Bale, Michael Bamshad, Deborah Barbouth, Pinar Bayrak-Toydemir, Anita Beck, Alan H. Beggs, Edward Behrens, Gill Bejerano, Jimmy Bennet, Beverly Berg-Rood, Jonathan A. Bernstein, Gerard T. Berry, Anna Bican, Stephanie Bivona, Elizabeth Blue, John Bohnsack, Carsten Bonnenmann, Devon Bonner, Lorenzo Botto, Brenna Boyd, Lauren C. Briere, Elly Brokamp, Gabrielle Brown, Elizabeth A. Burke, Lindsay C. Burrage, Manish J. Butte, Peter Byers, William E. Byrd, John Carey, Olveen Carrasquillo, Ta Chen Peter Chang, Sirisak Chanprasert, Hsiao-Tuan Chao, Gary D. Clark, Terra R. Coakley, Laurel A. Cobban, Joy D. Cogan, Matthew Coggins, F. Sessions Cole, Heather A. Colley, Cynthia M. Cooper, Heidi Cope, William J. Craigen, Andrew B. Crouse, Michael Cunningham, Precilla D'Souza, Hongzheng Dai, Surendra Dasari, Joie Davis, Jyoti G. Dayal, Matthew Deardorff, Esteban C. Dell'Angelica, Shweta U. Dhar, Katrina Dipple, Daniel Doherty, Naghmeh Dorrani, Argenia L. Doss, Emilie D. Douine, David D. Draper, Laura Duncan, Dawn Earl, David J. Eckstein, Lisa T. Emrick, Christine M. Eng, Cecilia Esteves, Marni Falk, Liliana Fernandez, Carlos Ferreira, Elizabeth L. Fieg, Laurie C. Findley, Paul G. Fisher, Brent L. Fogel, Irman Forghani, Laure Fresard, William A. Gahl, Ian Glass, Bernadette Gochuico, Rena A. Godfrey, Katie Golden-Grant, Alica M. Goldman, Madison P. Goldrich, David B. Goldstein, Alana Grajewski, Catherine A. Groden, Irma Gutierrez, Sihoun Hahn, Rizwan Hamid, Neil A. Hanchard, Kelly Hassey, Nichole Hayes, Frances High, Anne Hing, Fuki M. Hisama, Ingrid A. Holm, Jason Hom, Martha Horike-Pyne, Alden Huang, Yong Huang, Laryssa Huryn, Rosario Isasi, Fariha Jamal, Gail P. Jarvik, Jeffrey Jarvik, Suman Jayadev, Lefkothea Karaviti, Jennifer Kennedy, Dana Kiley, Shilpa N. Kobren, Isaac S. Kohane, Jennefer N. Kohler, Deborah Krakow, Donna M. Krasnewich, Elijah Kravets, Susan Korrick, Mary Koziura, Joel B. Krier, Seema R. Lalani, Byron Lam, Christina Lam, Grace L. LaMoure, Brendan C. Lanpher, Ian R. Lanza, Lea Latham, Kimberly LeBlanc, Brendan H. Lee, Hane Lee, Roy Levitt, Richard *A. Lewis*, Sharyn A. Lincoln, Pengfei Liu, Xue Zhong Liu, Nicola Longo, Sandra K. Loo, Joseph Loscalzo, Richard L. Maas, John MacDowall, Ellen F. Macnamara, Calum A. MacRae, Valerie V. Maduro, Marta M. Majcherska, Bryan C. Mak, May Christine V. Malicdan, Laura A. Mamounas, Teri A. Manolio, Rong Mao, Kenneth Maravilla, Thomas

C. Markello, Ronit Marom, Gabor Marth, Beth A. Martin, Martin G. Martin, Julian A. Martínez-Agosto, Shruti Marwaha, Jacob McCauley, Allyn McConkie-Rosell, Colleen E. McCormack, Alexa T. McCray, Elisabeth McGee, Heather Mefford, J. Lawrence Merritt, Matthew Might, Ghayda Mirzaa, Eva Morava, Paolo M. Moretti, Deborah Mosbrook-Davis, John J. Mulvihill, David R. Murdock, Anna Nagy, Mariko Nakano-Okuno, Avi Nath, Stan F. Nelson, John H. Newman, Sarah K. Nicholas, Deborah Nickerson, Shirley Nieves-Rodriguez, Donna Novacic, Devin Oglesbee, James P. Orengo, Laura Pace, Stephen C. Pak, J. Carl Pallais, Christina GS. Palmer, Jeanette C. Papp, Neil H. Parker, John A. Phillips III, Jennifer E. Posey, Lorraine Potocki, Bradley Power, Barbara N. Pusey, Aaron Quinlan, Wendy Raskind, Archana N. Raja, Deepak A. Rao, Genecee Renteria, Chloe M. Reuter, Lynette Rives, Amy K. Robertson, Lance H. Rodan, Jill A. Rosenfeld, Natalie Rosenwasser, Francis Rossignol, Maura Ruzhnikov, Ralph Sacco, Jacinda B. Sampson, Susan L. Samson, Mario Saporta, C. Ron Scott, Judy Schaechter, Timothy Schedl, Kelly Schoch, Daryl A. Scott, Vandana Shashi, Jimann Shin, Rebecca Signer, Edwin K. Silverman, Janet S. Sinsheimer, Kathy Sisco, Edward C. Smith, Kevin S. Smith, Emily Solem, Lilianna Solnica-Krezel, Ben Solomon, Rebecca C. Spillmann, Joan M. Stoler, Jennifer A. Sullivan, Kathleen Sullivan, Angela Sun, Shirley Sutton, David A. Sweetser, Virginia Sybert, Holly K. Tabor, Amelia L. M. Tan, Queenie K.-G. Tan, Mustafa Tekin, Fred Telischi, Willa Thorson, Audrey Thurm, Cynthia J. Tifft, Camilo Toro, Alyssa A. Tran, Brianna M. Tucker, Tiina K. Urv, Adeline Vanderver, Matt Velinder, Dave Viskochil, Tiphanie P. Vogel, Colleen E. Wahl, Stephanie Wallace, Nicole M. Walley, Chris A. Walsh, Melissa Walker, Jennifer Wambach, Jijun Wan, Lee-kai Wang, Michael F. Wangler, Patricia A. Ward, Daniel Wegner, Mark Wener, Tara Wenger, Katherine Wesseling Perry, Monte Westerfield, Matthew T. Wheeler, Jordan Whitlock, Lynne A. Wolfe, Jeremy D. Woods, Shinya Yamamoto, John Yang, Muhammad Yousef, Diane B. Zastrow, Wadih Zein, Chunli Zhao, Stephan Zuchner.

Declaration of Competing Interest

The authors declare that they have no conflict of interests.

Acknowledgements

References

[1] A. Wise, L. Tenezaca, R.W. Fernandez, E. Schatoff, J. Flores, A. Ueda, et al., Drosophila mutants of the autism candidate gene neurobeachin (rugose) exhibit neurodevelopmental disorders, aberrant synaptic properties, altered locomotion, and impaired adult social behavior and activity patterns, J. Neurogenet. 29 (2015) 135–143, https://doi.org/10.3109/01677063.2015.1064916.

[2] K. Volders, S. Scholz, J.R. Slabbaert, A.C. Nagel, P. Verstreken, J.W.M. Creemers, et al., Drosophila rugose is a functional homolog of mammalian Neurobeachin and affects synaptic architecture, brain morphology, and associative learning, J. Neurosci. 32 (2012) 15193–15204, https://doi.org/10.1523/JNEUROSCI.6424-11.2012.

[3] A.C. Miller, L.H. Voelker, A.N. Shah, C.B. Moens, Neurobeachin is required postsynaptically for electrical and chemical synapse formation, Curr. Biol. 25 (2015) 16–28, https://doi.org/10.1016/j.cub.2014.10.071.

[4] X. Wang, F.W. Herberg, M.M. Laue, C. Wullner, B. Hu, E. Petrasch-Parwez, et al., Neurobeachin: a protein kinase A-anchoring, beige/Chediak-higashi protein homolog implicated in neuronal membrane traffic, J. Neurosci. 20 (2000) 8551–8565.

[5] K. Niesmann, D. Breuer, J. Brockhaus, G. Born, I. Wolff, C. Reissner, et al., Dendritic spine formation and synaptic function require neurobeachin, Nat. Commun. 2 (2011) 557, https://doi.org/10.1038/ncomms1565.

[6] J. Lauks, P. Klemmer, F. Farzana, R. Karupothula, R. Zalm, N.E. Cooke, et al., Synapse associated protein 102 (SAP102) binds the C-terminal part of the scaffolding protein neurobeachin, PLoS One 7 (2012), e39420https://doi.org/10.1371/journal.pone.0039420.

[7] F. Farzana, R. Zalm, N. Chen, K.W. Li, S.G.N. Grant, A.B. Smit, et al., Neurobeachin regulates glutamate- and GABA-receptor targeting to synapses via distinct pathways, Mol. Neurobiol. 53 (2016) 2112–2123, https://doi.org/10.1007/s12035-015-9164-8.

[8] L. Medrihan, A. Rohlmann, R. Fairless, J. Andrae, M. Döring, M. Missler, et al., Neurobeachin, a protein implicated in membrane protein traffic and autism, is required for the formation and functioning of central synapses, J. Physiol. 587 (2009) 5095–5106, https://doi.org/10.1113/jphysiol.2009.178236.

[9] R. Nair, J. Lauks, S. Jung, N.E. Cooke, H. de Wit, N. Brose, et al., Neurobeachin regulates neurotransmitter receptor trafficking to synapses, J. Cell Biol. 200 (2013) 61–80, https://doi.org/10.1083/jcb.201207113.

[10] M. Smith, A. Woodroffe, R. Smith, S. Holguin, J. Martinez, P.A. Filipek, et al., Molecular genetic delineation of a deletion of chromosome 13q12–>q13 in a patient with autism and auditory processing deficits, Cytogenet. Genome Res. 98 (2002) 233–239, https://doi.org/10.1159/000071040.

[11] D. Castermans, V. Wilquet, E. Parthoens, C. Huysmans, J. Steyaert, L. Swinnen, et al., The neurobeachin gene is disrupted by a translocation in a patient with idiopathic autism, J. Med. Genet. 40 (2003) 352–356, https://doi.org/10.1136/jmg.40.5.352.

[12] M. Miura, A. Ishiyama, E. Nakagawa, M. Sasaki, K. Kurosawa, K. Inoue, et al., 13q13.3 microdeletion associated with apparently balanced translocation of 46,XX,t(7;13) suggests NBEA involvement, Brain Dev. 42 (2020) 581–586, https://doi.org/10.1016/j.braindev.2020.05.006.

[13] M.S. Mulhern, C. Stumpel, N. Stong, H.G. Brunner, L. Bier, N. Lippa, et al., NBEA: developmental disease gene with early generalized epilepsy phenotypes, Ann. Neurol. 84 (2018) 788–795, https://doi.org/10.1002/ana.25350.

[14] M.F. Wangler, S. Yamamoto, H.-T. Chao, J.E. Posey, M. Westerfield, J. Postlethwait, et al., Model organisms facilitate rare disease diagnosis and therapeutic research, Genetics. 207 (2017) 9–27, https://doi.org/10.1534/genetics.117.203067.

[15] D.G. MacArthur, T.A. Manolio, D.P. Dimmock, H.L. Rehm, J. Shendure, G.R. Abecasis, et al., Guidelines for investigating causality of sequence variants in human disease, Nature. 508 (2014) 469–476, https://doi.org/10.1038/nature13127.

[16] S. Richards, N. Aziz, S. Bale, D. Bick, S. Das, J. Gastier-Foster, et al., Standards and guidelines for the interpretation of sequence variants: a joint consensus recommendation of the American College of Medical Genetics and Genomics and the Association for Molecular Pathology, Genet Med (2015) 405–424, https://doi.org/10.1038/gim.2015.30.

[17] W.A. Gahl, J.J. Mulvihill, C. Toro, T.C. Markello, A.L. Wise, R.B. Ramoni, et al., The NIH undiagnosed diseases program and network: applications to modern medicine, Mol. Genet. Metab. 117 (2016) 393–400, https://doi.org/10.1016/j.ymgme.2016.01.007.

[18] W.A. Gahl, A.L. Wise, E.A. Ashley, The undiagnosed diseases network of the National Institutes of Health: a National Extension, Jama. 314 (2015) 1797–1798, https://doi.org/10.1001/jama.2015.12249.

[19] R.B. Ramoni, J.J. Mulvihill, D.R. Adams, P. Allard, E.A. Ashley, J.A. Bernstein, et al., The undiagnosed diseases network: accelerating discovery about health and disease, Am. J. Hum. Genet. 100 (2017) 185–192, https://doi.org/10.1016/j.ajhg.2017.01.006.

[20] S.E. Brnich, A.N. Abou Tayoun, F.J. Couch, G.R. Cutting, M.S. Greenblatt, C.D. Heinen, et al., Recommendations for application of the functional evidence PS3/BS3 criterion using the ACMG/AMP sequence variant interpretation framework, Genome Med. 12 (2019) 3–12, https://doi.org/10.1186/s13073-019-0690-2.

[21] S. Brenner, The genetics of Caenorhabditis elegans, Genetics. 77 (1974) 71–94, https://doi.org/10.1016/j.bbrc.2017.09.147.

[22] W.H. Tsang, K.F. Shek, T.Y. Lee, K.L. Chow, An evolutionarily conserved nested gene pair - Mab21 and Lrba/Nbea in metazoan, Genomics. 94 (2009) 177–187, https://doi.org/10.1016/j.ygeno.2009.05.009.

[23] C. Martínez Jaramillo, C.M. Trujillo-Vargas, LRBA in the endomembrane system, Colomb Med (Cali) 49 (2018) 236–243, https://doi.org/10.25100/cm.v49i2.3802.

[24] N. de Souza, L.G. Vallier, H. Fares, I. Greenwald, SEL-2, the *C. elegans* neurobeachin/LRBA homolog, is a negative regulator of lin-12/Notch activity and affects endosomal traffic in polarized epithelial cells, Development 134 (2007) 691–702, https://doi.org/10.1242/dev.02767.

[25] A. Paix, A. Folkmann, D. Rasoloson, G. Seydoux, High efficiency, homology-directed genome editing in Caenorhabditis elegans using CRISPR-Cas9 ribonucleoprotein complexes, Genetics. 201 (2015) 47–54, https://doi.org/10.1534/genetics.115.179382.

[26] C. Frøkjær-Jensen, M.W. Davis, M. Sarov, J. Taylor, S. Flibotte, M. LaBella, et al., Random and targeted transgene insertion in Caenorhabditis elegans using a modified Mos1 transposon, Nat Meth. 11 (2014) 529–534, https://doi.org/10.1038/nmeth.2889.

[27] S. El Mouridi, C. Lecroisey, P. Tardy, M. Mercier, A. Leclercq-Blondel, N. Zariohi, et al., Reliable CRISPR/Cas9 Genome Engineering in *Caenorhabditis elegans* Using a Single Efficient sgRNA and an Easily Recognizable Phenotype, G3 (Bethesda), 7, 2017 1429–1437, https://doi.org/10.1534/g3.117.040824.

[28] D.J. Dickinson, A.M. Pani, J.K. Heppert, C.D. Higgins, B. Goldstein, Streamlined genome engineering with a self-excising drug selection cassette, Genetics. 200 (2015) 1035–1049, https://doi.org/10.1534/genetics.115.178335.

[29] P.W. Sternberg, Vulval development, WormBook. (2005) 1–28, https://doi.org/10.1895/wormbook.1.6.1.

[30] P. Enyedi, G. Czirják, Molecular background of leak K+ currents: two-pore domain potassium channels, Physiol. Rev. 90 (2010) 559–605, https://doi.org/10.1152/physrev.00029.2009.

[31] I. Ben Soussia, S. El Mouridi, D. Kang, A. Leclercq-Blondel, L. Khoubza, P. Tardy, et al., Mutation of a single residue promotes gating of vertebrate and invertebrate two-pore domain potassium channels, Nat. Commun. 10 (2019) 787, https://doi.org/10.1038/s41467-019-08710-3.

[32] J. Cao, J.S. Packer, V. Ramani, D.A. Cusanovich, C. Huynh, R. Daza, et al., Comprehensive single-cell transcriptional profiling of a multicellular organism, Science. 357 (2017) 661–667, https://doi.org/10.1126/science.aam8940.

[33] J. Muellerleile, A. Blistein, A. Rohlmann, F. Scheiwe, M. Missler, S.W. Schwarzacher, et al., Enhanced LTP of population spikes in the dentate gyrus of mice haploinsufficient for neurobeachin, Sci. Rep. 10 (2020)https://doi.org/10.1038/s41598-020-72925-4 16058–12.

[34] K.M. Bowling, M.L. Thompson, M.D. Amaral, C.R. Finnila, S.M. Hiatt, K.L. Engel, et al., Genomic diagnosis for children with intellectual disability and/or developmental delay, Genome Med. 9 (2017) 43, https://doi.org/10.1186/s13073-017-0433-1.

[35] I. Iossifov, B.J. O'Roak, S.J. Sanders, M. Ronemus, N. Krumm, D. Levy, et al., The contribution of de novo coding mutations to autism spectrum disorder, Nature. 515 (2014) 216–221, https://doi.org/10.1038/nature13908.

[36] D. Repetto, J. Brockhaus, H.J. Rhee, C. Lee, M.W. Kilimann, J. Rhee, et al., Molecular dissection of Neurobeachin function at excitatory synapses, Front Synaptic Neurosci. 10 (2018) 28, https://doi.org/10.3389/fnsyn.2018.00028.

[37] K. Tuand, P. Stijnen, K. Volders, J. Declercq, K. Nuytens, S. Meulemans, et al., Nuclear localization of the autism candidate gene Neurobeachin and functional interaction with the NOTCH1 intracellular domain indicate a role in regulating transcription, PLoS One 11 (2016), e0151954https://doi.org/10.1371/journal.pone.0151954.

[38] I. del Pino, I. Paarmann, M. Karas, M.W. Kilimann, H. Betz, The trafficking proteins Vacuolar protein sorting 35 and Neurobeachin interact with the glycine receptor β-subunit, Biochem. Biophys. Res. Commun. 412 (2011) 435–440, https://doi.org/10.1016/j.bbrc.2011.07.110.

[39] O. Barel, S.A. Shalev, R. Ofir, A. Cohen, J. Zlotogora, Z. Shorer, et al., Maternally inherited Birk Barel mental retardation dysmorphism syndrome caused by a mutation in the genomically imprinted potassium channel KCNK9, Am. J. Hum. Genet. 83 (2008) 193–199, https://doi.org/10.1016/j.ajhg.2008.07.010.

[40] M. Šedivá, P. Lašš́uthová, J. Záměčník, L. Sedláčková, P. Seeman, J. Haberlová, Novel variant in the KCNK9 gene in a girl with Birk Barel syndrome, Eur J Med Genet. 63 (2020) 103619, https://doi.org/10.1016/j.ejmg.2019.01.009.